Sample-to-sample fluctuations of electrostatic forces generated by quenched charge disorder

David S. Dean,[1] Ali Naji,[2] and Rudolf Podgornik[3,4]

[1]*Laboratoire de Physique Théorique (IRSAMC),Université de Toulouse, UPS and CNRS, F-31062 Toulouse, France*
[2]*Department of Applied Mathematics and Theoretical Physics, Centre for Mathematical Sciences, University of Cambridge,*
Cambridge CB3 0WA, United Kingdom
[3]*Department of Theoretical Physics, J. Stefan Institute, SI-1000 Ljubljana, Slovenia*
[4]*Institute of Biophysics, School of Medicine and Department of Physics, Faculty of Mathematics and Physics, University of Ljubljana,*
SI-1000 Ljubljana, Slovenia

It has been recently shown that randomly charged surfaces can exhibit-long range electrostatic interactions even when they are net neutral. These forces depend on the specific realization of charge disorder and thus exhibit sample-to-sample fluctuations about their mean value. We analyze the fluctuations of these forces in the parallel slab configuration and in the sphere-plane geometry via the proximity force approximation. The fluctuations of the normal forces, which have a finite mean value, are computed exactly. Surprisingly, we also show that fluctuations in lateral forces are present, despite the fact that they have a zero mean, and that they have the same scaling behavior as the normal force fluctuations. The measurement of these lateral force fluctuations could help us to characterize the effects of charge disorder in experimental systems, leading to estimates of their magnitudes that are complementary to those given by normal force measurements.

PACS number(s): 05.40.−a, 34.20.Gj, 03.50.De

I. INTRODUCTION

Stability of soft and biological matter in particular is mostly an outcome of the equilibrium between variable-range Coulomb and long-range van der Waals-Casimir interactions that feature in many contexts [1]. Though direct measurements of the latter have been announced by various experimental groups, the details and the accuracy of experiments are sometimes questioned by the experimenters themselves [2]. Over the last few years there have been increasing concerns over how to effectively differentiate between the long-range Coulomb interactions and the long-range van der Waals-Casimir interactions in experiments on interactions between metallic bodies *in vacuo* [3]. A number of authors have pointed out that disorder effects may significantly affect the forces between surfaces in such experiments; possible sources of disorder include the random surface electrostatic potential [4] connected with the so-called *patch effect* due to the variation of local crystallographic axes of the exposed surface of a clean polycrystalline sample [5], as well as effects of disorder in the local dielectric constant [6]. The direct detection of disorder effects in Casimir force experiments, when the force is measured as a function of the intersurface separation of two plates, or in standard manner between a plate and a sphere, is difficult as they must be unraveled from other forces that are always present [3].

Recently it has been proposed that quenched random-charge disorder on surfaces as well as in the bulk can lead to long-range interactions even when the surfaces are net neutral [7,8]. These long-range interactions are induced by a subtle image charge effect, and they could play a significant role in experiments to measure the Casimir force as well as in colloidal science in general [9], where, for instance, random surface charging can occur during preparation of surfactant-coated surfaces [10]. Other examples of objects bearing random charge are random polyelectrolytes and polyampholytes [11].

Although in the latter case the charge distribution could be quenched (i.e., intrinsic to the chain assembly during the polymerization process) or annealed (i.e., when monomers have weak acidic or basic groups that can charge regulate depending on the pH of the solution), it is not unequivocal to asses the nature of the charge disorder distribution in the case of surfactant-coated surfaces. The statistics of the random lateral potential between randomly charged plates and rods has been studied [12], and the roughness of the resulting energy landscape can lead to novel stick slip and frictional behavior [12,13]. When randomly charged surfaces and objects are free to move laterally and rotate with respect to each other, prealignment phenomena can occur at a distance and can aid the objects to come into close contact [12]. Clearly the apparent disorder seen in complex biological molecules will play an important role in their interactions, and the precise distribution of interacting sites on their surface may play an important functional role. Indeed, in the case of generic pairwise interactions between atoms randomly distributed on surfaces, as occurs in simple models for proteins, the degree of self-attraction can be increased by correlating the distribution of the atoms on each surface [14].

In this paper we show that net-neutral surfaces experience two types of disorder-generated forces that thus show pronounced sample-to-sample fluctuations. The first disorder-generated force is normal to the interacting surfaces, whose features we have already investigated in detail elsewhere [7], and shows a nonzero average and fluctuations proportional to the average. The second one, addressed in detail here, is the lateral disorder-generated force, acting within the plane parallel to that of the interacting surfaces, whose average is zero but nevertheless exhibits sample-to-sample fluctuations that can be quite large. In principle, measurements of lateral force fluctuations could be useful in characterizing and unraveling the effects of quenched charge disorder and thus help the analysis of its role in normal force measurements.
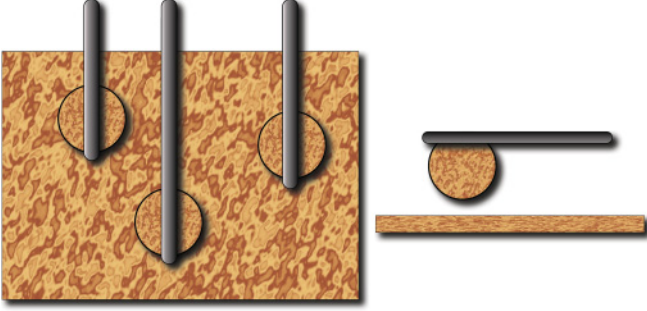
FIG. 1. (Color online) A schematic top view of a spherical atomic force microscopy (AFM) tip (right: side view) with disordered charge distribution above a planar substrate with similar charge distribution. Three different realizations of the experiment, i.e., three different lateral positions of the tip above the substrate, are shown corresponding to three different samples of force data. Each sample would show a different measurement of the normal as well as lateral force with a sample-to-sample variance calculated in the main text.

To give an example of how these forces could be measured, one could take a small randomly charged slab at some distance l from another slab and place its center randomly at some position opposite the larger slab. The same could be done rather more effectively with a plane and a sphere as schematically shown in Fig. 1. Now, due to the nonhomogeneous quenched charge distribution, the smaller slab will experience a random lateral force varying from sample to sample. Such forces could conceivably be readily measurable in an surface force apparatus (SFA)-type setup [15] used to measure shear forces between solid surfaces sliding past each other across aqueous salt solutions [16] but with interacting surfaces bearing disordered charge distribution. The lateral forces measured in distinct experiments varying in regard to the exact relative lateral positions between the interacting surfaces will average out to zero, but we predict that the fluctuations of this lateral force are nonzero and can give information about the magnitude of charge disorder in the system. The fluctuations we compute here thus correspond to sample-to-sample fluctuations and stem from different sample (experiment) specific relative positions of the interacting surfaces in different experiments. These fluctuations are thus distinct from the temporal fluctuations in the measured force due to thermal fluctuations (an example being thermal fluctuations of the instantaneous thermal Casimir force as discussed in Ref. [17]).

Most of our computations are for the slab geometry where they can be carried out exactly; however, we show how the lateral force fluctuations can be approximately computed also in the case of the sphere-plane geometry shown in Fig. 1. This configuration is an adaptation of the setup standardly assumed to be within the reach of the *proximity force approximation* (PFA) [18], or equivalently the *Deryaguin force approximation* [19], in the case where the charge disorder on the sphere is assumed to be uncorrelated or very weakly correlated. Using an alternative calculational method where there is no dielectric discontinuity (i.e., all materials used and the intervening space between them have the same dielectric constant), we can compute the lateral force fluctuations exactly for the sphere-plane system. The form of the PFA developed here

agrees with this exact computation in this limit. For the slab geometry, we find that the lateral force fluctuations (lateral force variance) behave as A/l^2 where A is the area of the smaller slab and l is the slab separation. In the sphere-plane setup, within the PFA we find that the lateral force fluctuations behave as R/l, where R is the radius of the sphere, and we take the limit where $R \gg l$, with l being the closest distance of the sphere to the plane.

For completeness we give the expression for lateral force fluctuations in the case where the intervening medium is an electrolyte described in the weak-coupling Debye-Hückel approximation [20] as well. In this case the force fluctuations are exponentially screened with a screening length given by the Debye length.

We then turn to the computation of the normal force fluctuations. The method used here is slightly different from in normal force fluctuations since there is a contribution from image charges whose average is in general nonzero. We reproduce the results of Refs. [7,8] for the average normal force using this method and then go on to analyze its fluctuations. For the slab geometry with no electrolyte present, we show that the normal force behaves as A/l^2, while its variance also scales as A/l^2, making both of them comparable. In the sphere-plane setup, we find that the fluctuations of the normal force relative to its average value vary as $\sqrt{l/R}$ and thus become increasingly more important as the separation is increased.

II. LATERAL FORCE FLUCTUATIONS

Consider two parallel infinite slabs separated by a distance l. The slab whose surface is at $z = 0$ has a dielectric constant ϵ_2, and the slab whose surface is at $z = l$ has a dielectic constant ϵ_1. We call these slabs S_2 and S_1, respectively (see Fig. 2). We denote by ϵ_m the dielectric constant of the intervening material. Let each slab have a random surface charge density $\rho_\alpha(\mathbf{x}) = \rho_\alpha(\mathbf{r}, z)$ with zero mean (i.e., the surfaces are net neutral) and correlation function in the plane of the slabs ($\mathbf{r}, \mathbf{r}' \in S_1, S_2$):

$$\langle \rho_\alpha(\mathbf{r}, z)\rho_\beta(\mathbf{r}', z')\rangle = \delta_{\alpha\beta} g_{\alpha s}\delta(z - l_\alpha)\delta(z' - l_\beta)C_\alpha(\mathbf{r} - \mathbf{r}'),$$
$$\alpha, \beta = 1, 2, \tag{1}$$

and where we define $l_2 = 0$ and $l_1 = l$. In addition we assume that the charge distribution on slab S_1 is restricted to a finite
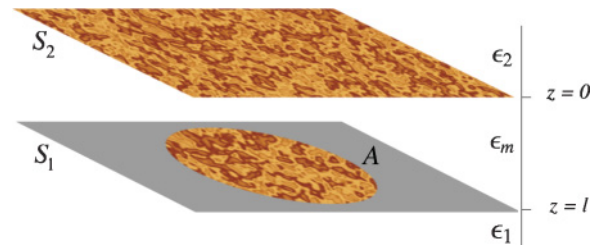

FIG. 2. (Color online) A schematic view of the bounding surfaces of two parallel semi-infinite slabs separated by a distance l. The surfaces are net neutral but carry a finite amount of quenched charge disorder. The slab (S_2) whose surface is at $z = 0$ has a dielectric constant ϵ_2, and the slab (S_1) whose surface is at $z = l$ has a dielectic constant ϵ_1. We denote by ϵ_m the dielectric constant of the intervening material. In general, we assume that the charge distribution on slab S_1 is restricted to a finite area A; we then take the limit of large A.

area A. In the case where the random charge is made up of point charges of signs $\pm e$ of surface density $n_{\alpha s}$ we can write $g_{\alpha s} = e^2 n_{\alpha s}$, and the correlation function $C_\alpha(\mathbf{r} - \mathbf{r}')$ has dimensions of inverse length squared, meaning that its two-dimensional Fourier transform is dimensionless. Typically the values of n_s for quite pure samples are smaller than the bulk disorder variance, which has a typical range between 10^{-11} to 10^{-6} nm^{-3} (corresponding to impurity charge densities of 10^{10} to 10^{15} $e/$cm^3 [7]).

The electrostatic energy of the system is given by

$$E = \frac{1}{2} \int d\mathbf{x}\phi(\mathbf{x})\rho(\mathbf{x}), \tag{2}$$

where $\rho(\mathbf{x})$ is the total charge density and $\phi(\mathbf{x})$ is the electrostatic potential, which is given by

$$\phi(\mathbf{x}) = \int d\mathbf{y}G(\mathbf{x},\mathbf{y})\rho(\mathbf{y}), \tag{3}$$

while $G(\mathbf{x},\mathbf{y})$ is Green's function obeying

$$\epsilon_0 \nabla \cdot \epsilon(\mathbf{x})\nabla G(\mathbf{x},\mathbf{y}) = -\delta(\mathbf{x} - \mathbf{y}), \tag{4}$$

with $\epsilon(\mathbf{x})$ the local dielectric function. Upon changing the charge distribution the corresponding change in the energy of the system is thus given by

$$\delta E = \int d\mathbf{x}d\mathbf{y}\delta\rho(\mathbf{x})G(\mathbf{x},\mathbf{y})\rho(\mathbf{y}). \tag{5}$$

If ρ_1, the charge distribution on the slab S_1, is made up of point charges, we have

$$\rho_1(\mathbf{x}) = \sum_{n \in S_1} q_n \delta(\mathbf{x} - \mathbf{x}_n), \tag{6}$$

where q_n is the charge at the site $\mathbf{x}_n$. Now, on moving the smaller slab S_1 by a distance $\mathbf{a}$ laterally, i.e., normally to the normal between slabs, we find that the new charge distribution is simply given by

$$\rho_1'(\mathbf{x}) = \sum_{n \in S_1} q_n \delta(\mathbf{r} - \mathbf{r}_n - \mathbf{a})\delta(z - z_n). \tag{7}$$

This means that we can write

$$\delta\rho(\mathbf{x}) = \delta\rho_1(\mathbf{x}) = -\mathbf{a} \cdot \nabla_\mathbf{r}\rho_1(\mathbf{r},z). \tag{8}$$

As the plate S_1 is moved laterally the self-interaction between the charges in both plates is unchanged, thus the energy change is given only by the interaction of the charges and image charges in S_1 with those in S_2. We may thus write

$$\delta E = -\mathbf{a} \cdot \int d\mathbf{r}'d\mathbf{r}dzdz'\nabla_{\mathbf{r}'}\rho_1(\mathbf{r}',z')G(\mathbf{r} - \mathbf{r}';z,z')\rho_2(\mathbf{r},z), \tag{9}$$

where $\mathbf{r}'$ and $\mathbf{r}$ are again the two-dimensional coordinates in the planes of S_1 and S_2, respectively, and z' and z are the respective coordinates normal to the planes. We thus note that the integration over the coordinate $\mathbf{r}'$ is over a finite area A, while that over $\mathbf{r}$ is unrestricted. The lateral force $\mathbf{F}^{(L)}$ on plate S_1 is thus given by

$$\delta E = -\mathbf{a} \cdot \mathbf{F}^{(L)}. \tag{10}$$

As the charges in plates S_1 and S_2 are uncorrelated, we find that

$$\langle \delta E \rangle = -\langle \mathbf{a} \cdot \mathbf{F}^{(L)} \rangle = 0; \tag{11}$$

that is, the average lateral force is zero.

The variance of the energy change is given by

$$\langle \delta E^2 \rangle = a_i a_j \bigg\langle \int d\mathbf{r}'d\mathbf{r}dzdz'd\mathbf{s}'d\mathbf{s}d\zeta d\zeta' \nabla_{\mathbf{r}_i'}\rho_1(\mathbf{r}',z')$$
$$\times G(\mathbf{r} - \mathbf{r}';z,z')\rho_2(\mathbf{r},z)\nabla_{\mathbf{s}_j'}\rho_1(\mathbf{s}',\zeta')$$
$$\times G(\mathbf{s} - \mathbf{s}';\zeta,\zeta')\rho_2(\mathbf{s},\zeta) \bigg\rangle, \tag{12}$$

where the summation is over the in-plane Cartesian components $i, j = 1,2$. As the charge distributions on the two slabs are independent, the only nonzero correlations here are given by

$$\langle \rho_2(\mathbf{r},z)\rho_2(\mathbf{s},\zeta) \rangle = g_{2s}\delta(z)\delta(\zeta)C_2(\mathbf{r} - \mathbf{s}), \tag{13}$$

$$\big\langle \nabla_{\mathbf{r}_i'}\rho_1(\mathbf{r}',z')\nabla_{\mathbf{s}_j'}\rho_1(\mathbf{s}',\zeta') \big\rangle$$
$$= g_{1s}\delta(z' - l)\delta(\zeta' - l)\nabla_{\mathbf{r}_i'}\nabla_{\mathbf{s}_j'}C_1(\mathbf{r}' - \mathbf{s}'). \tag{14}$$

This then yields

$$\langle \delta E^2 \rangle = a_i a_j g_{1s}g_{2s} \int d\mathbf{r}'d\mathbf{r}d\mathbf{s}'d\mathbf{s}\, G(\mathbf{r} - \mathbf{r}';0,l)G(\mathbf{s} - \mathbf{s}';0,l)$$
$$\times C_2(\mathbf{r} - \mathbf{s})\nabla_{\mathbf{r}_i'}\nabla_{\mathbf{s}_j'}C_1(\mathbf{r}' - \mathbf{s}'). \tag{15}$$

We now write this equation in terms of the two-dimensional Fourier transforms, with respect to the in-plane coordinates $\tilde{G}$ and $\tilde{C}$ of the functions G and C and carry out the integrations over the unrestricted coordinates $\mathbf{r}$ and $\mathbf{s}$ to find

$$\langle \delta E^2 \rangle = \frac{a_i a_j g_{1s}g_{2s}}{(2\pi)^4} \int d\mathbf{k}d\mathbf{q}d\mathbf{r}'d\mathbf{s}'\, q_i q_j \tilde{G}(k;0,l)^2 \tilde{C}_2(k)$$
$$\times \tilde{C}_1(q)e^{i(\mathbf{q}-\mathbf{k})\cdot(\mathbf{r}'-\mathbf{s}')}, \tag{16}$$

where we have used the fact that $\tilde{G}(\mathbf{k};0,l)$ and $\tilde{C}_\alpha(\mathbf{k})$ are functions of $|\mathbf{k}| = k$ only. Now using the fact that the surface charge patch (of area A) on slab S_1 is large and assuming that the correlations between charges are sufficiently short range, we may write

$$\langle \delta E^2 \rangle = \frac{Aa_i a_j g_{1s}g_{2s}}{(2\pi)^2} \int d\mathbf{k}k_i k_j \tilde{G}(k;0,l)^2 \tilde{C}_1(k)\tilde{C}_2(k)$$
$$= \frac{Aa^2 g_{1s}g_{2s}}{4\pi} \int dk k^3 \tilde{G}(k;0,l)^2 \tilde{C}_1(k)\tilde{C}_2(k), \tag{17}$$

where we have used the isotropy of the k integral. From this we deduce that

$$\big\langle F_i^{(L)} F_j^{(L)} \big\rangle = \frac{A\delta_{ij} g_{1s}g_{2s}}{4\pi} \int dk k^3 \tilde{G}(k;0,l)^2 \tilde{C}_1(k)\tilde{C}_2(k). \tag{18}$$

The Fourier transform of Green's function for the parallel slab configuration is easily computed by standard methods and is given by

$$\tilde{G}(k;0,l) = \frac{2\epsilon_m \exp(-kl)}{k\epsilon_0(\epsilon_m + \epsilon_1)(\epsilon_m + \epsilon_2)[1 - \Delta_1\Delta_2 \exp(-2kl)]}, \tag{19}$$

where

$$\Delta_\alpha = \frac{\epsilon_\alpha - \epsilon_m}{\epsilon_\alpha + \epsilon_m}, \quad \alpha = 1,2, \tag{20}$$

giving the general result in the form

$$\langle F_i^{(L)} F_j^{(L)} \rangle = \frac{A \delta_{ij} g_{1s} g_{2s} \epsilon_m^2}{\pi \epsilon_0^2 (\epsilon_m + \epsilon_1)^2 (\epsilon_m + \epsilon_2)^2}$$
$$\times \int k \, dk \, \frac{\exp(-2kl) \tilde{C}_1(k) \tilde{C}_2(k)}{[1 - \Delta_1 \Delta_2 \exp(-2kl)]^2}. \tag{21}$$

To go further we must specify the form of spatial charge disorder. For large interslab separations l the expression (21) is dominated by the integrand at small values of k. The large distance behavior of the force fluctuations (and indeed the force) thus depends on the functions $\tilde{C}_{1/2}(k)$ near $k = 0$. If both of these correlation functions are nonzero at $k = 0$, then this means that the total net charge on each plate is zero on average but can fluctuate. In this case the long-range force fluctuations for charge distributions of correlation lengths ξ_α will be the same as that for uncorrelated charge disorder with $C_\alpha(\mathbf{r} - \mathbf{r}') = \tilde{C}_\alpha(0) \delta(\mathbf{r} - \mathbf{r}')$. However, when the distance l becomes of the same order of ξ_1 or ξ_2, the force fluctuations will become sensitive to the precise form of the charge distribution correlation function. Another type of disorder one can consider is random dipolar disorder, where dipoles rather than point charges are placed randomly on the surfaces. For this form of charge disorder there is no net statistical charge on the surface, and we have $\tilde{C} \sim p_0^2 k^2$, where p_0 is the length of the dipole (assuming the two partial charges are proportional to e). The analysis of the rest of this paper can easily be extended to this case, and it is easy to see that the power laws for the force and its fluctuations are modified, decaying by an additional factor of $1/l^2$ for each surface having dipolar charge disorder (the various prefactors are also modified). In what follows we shall restrict ourselves to the case of uncorrelated charge disorder, because the forces induced by the type of distribution with $\tilde{C}(0) \neq 0$ have the longest range and because, within this class, the long-range forces have a universal asymptotic form (independent of the correlation length).

When the spatial disorder correlations in both slabs are short range such that $C_\alpha(\mathbf{r} - \mathbf{r}') = \delta(\mathbf{r} - \mathbf{r}')$, we obtain

$$\langle F_i^{(L)} F_j^{(L)} \rangle = -\frac{A \delta_{ij} g_{1s} g_{2s} \epsilon_m^2}{4\pi \epsilon_0^2 l^2 (\epsilon_m + \epsilon_1)^2 (\epsilon_m + \epsilon_2)^2 \Delta_1 \Delta_2}$$
$$\times \ln(1 - \Delta_1 \Delta_2), \tag{22}$$

which shows that the lateral force fluctuations decay as A/l^2. We may rewrite this result as

$$\langle F_i^{(L)} F_j^{(L)} \rangle \equiv -\frac{A \delta_{ij} g_{1s} g_{2s}}{4\pi \epsilon_0^2 \epsilon_m^2 l^2} f\left(\frac{\epsilon_1}{\epsilon_m}, \frac{\epsilon_2}{\epsilon_m}\right), \tag{23}$$

where the function $f(\epsilon_1/\epsilon_m, \epsilon_2/\epsilon_m)$ follows directly from Eq. (22). It is plotted in Fig. 3 as a function of ϵ_1/ϵ_m and ϵ_2/ϵ_m. As can be easily ascertained, the lateral force fluctuations become weaker as $\epsilon_\alpha/\epsilon_m$ tends to infinity [in this case one can see that the function $f(x,y)$ decays, for instance, as $f(x,x) \sim \ln x/x^4$ and $f(x,0) \sim 1/x^2$ when $x \to \infty$], which corresponds to the case with perfect metallic slabs. On the other hand, when the dielectric constant of the intervening medium is increased, the force fluctuations become more
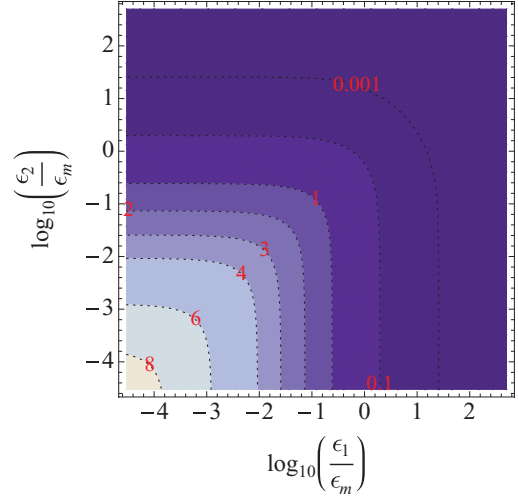

FIG. 3. (Color online) Contour plot of the rescaled lateral force fluctuations, $f(\epsilon_1/\epsilon_m, \epsilon_2/\epsilon_m)$ [Eqs. (22) and (23)], between two parallel slabs carrying quenched charge disorder as a function of ϵ_1/ϵ_m and ϵ_2/ϵ_m shown here on a $\log_{10} - \log_{10}$ scale.

pronounced and eventually diverge when both ϵ_1/ϵ_m and $\epsilon_2/\epsilon_m \to 0$ [exhibiting a logarithmic divergence, for instance, as $f(x,x) \sim -\ln x$ when $x \to 0$].

This result means that statistically the lateral force behaves as

$$F_i^{(L)} \sim \frac{\sqrt{A}}{l}. \tag{24}$$

Another interesting point here is that the lateral force fluctuations are also present when there are no dielectric discontinuities in the system. Here if we set $\epsilon_2 = \epsilon_1 = \epsilon_m$, we obtain the result

$$\langle F_i^{(L)} F_j^{(L)} \rangle = \frac{A \delta_{ij} g_{1s} g_{2s}}{64\pi \epsilon_0^2 \epsilon_m^2 l^2}. \tag{25}$$

This result can be derived in a rather straightforward but illuminating manner that we derive in the Appendix.

In the case where the intervening medium is composed of an electrolyte with dielectric constant ϵ_m and with inverse screening length m in the Debye-Hückel approximation, we find that the Green's function obeys

$$\epsilon_0 \nabla \cdot \epsilon(\mathbf{x}) \nabla G(\mathbf{x}, \mathbf{y}) - \epsilon_0 \epsilon(\mathbf{x}) \kappa^2(\mathbf{x}) G(\mathbf{x}, \mathbf{y}) = -\delta(\mathbf{x} - \mathbf{y}), \tag{26}$$

where as before $\epsilon(\mathbf{x})$ is only a function of z and $\kappa(\mathbf{x})$ is only nonzero (and equal to a constant κ) within the medium between the two slabs. From this we obtain

$$\tilde{G}(k; 0, l)$$
$$= \frac{2\epsilon_m K \exp(-Kl)}{\epsilon_0(\epsilon_m K + \epsilon_1 k)(\epsilon_m K + \epsilon_2 k)[1 - \Delta_{1\kappa} \Delta_{2\kappa} \exp(-2Kl)]}, \tag{27}$$

where $K = \sqrt{k^2 + \kappa^2}$ and

$$\Delta_{\alpha\kappa} = \frac{\epsilon_\alpha k - \epsilon_m K}{\epsilon_\alpha k + \epsilon_m K}, \qquad \alpha = 1,2. \tag{28}$$

In order to obtain the force fluctuations for a system with an intervening electrolyte, at the level of the Debye-Hückel approximation, we simply need to use the expression (27) in Eq. (18).

A. PFA for lateral forces

In many experimental setups, due to problems of achieving a perfectly parallel alignment, a sphere-plane configuration is used rather than a plane-parallel configuration. The derivation we have given is easily modified to the case of general geometries if one assumes the validity of the PFA [18]. In the case where there is no dielectric discontinuity, however, we can compute the lateral force fluctuations exactly for the sphere-plane geometry. We find in that case that for the sphere-plane geometry the force correlator is given by

$$\left\langle F_i^{(L)} F_j^{(L)} \right\rangle = \frac{\delta_{ij} g_{1s} g_{2s}}{32\pi^2 \epsilon_0^2 \epsilon_m^2} \int dS_1 dS_2 \frac{(\mathbf{x} - \mathbf{y})^2}{[(\mathbf{x} - \mathbf{y})^2 + z(\mathbf{x}, \mathbf{y})^2]^3}, \quad (29)$$

where $\mathbf{x}$ are the Cartesian coordinates on surface S_1 of object 1 (here the surface of a sphere of radius R) projected onto the in-plane coordinates of surface 2 and $\mathbf{y}$ the coordinates on surface 2 or S_2 (here an infinite plate). The variable $z(\mathbf{x}, \mathbf{y})$ is the distance between the points on the two surfaces perpendicular to the surface S_2. In terms of spherical polar coordinates on the surface S_1, if $\mathbf{x} = (R \sin\theta \cos\varphi, R \sin\theta \sin\varphi)$, then we have $z(\mathbf{x}, \mathbf{y}) = l + R(1 - \cos\theta)$, where l is the distance between the opposing pole of S_1 and the plane S_2 (or the closest distance of the sphere to the plane). The integral can now be written as

$$\left\langle F_i^{(L)} F_j^{(L)} \right\rangle = \frac{\delta_{ij} g_{1s} g_{2s}}{32\pi^2 \epsilon_0^2 \epsilon_m^2} \int R^2 \sin\theta \, d\theta \, d\phi \, d\mathbf{z}$$
$$\times \frac{\mathbf{z}^2}{[\mathbf{z}^2 + (l + R(1 - \cos\theta))^2]^3}, \quad (30)$$

where $\mathbf{z}$ is the relative coordinates of S_1 and S_2 in the plane of S_2 (i.e., it represents $\mathbf{x} - \mathbf{y}$, where $\mathbf{x}$ is in the plane of S_1 and $\mathbf{y}$ in the plane of S_2). Performing the integral over $\mathbf{z}$ we then find

$$\left\langle F_i^{(L)} F_j^{(L)} \right\rangle = \frac{\delta_{ij} g_{1s} g_{2s} R^2}{32\epsilon_0^2 \epsilon_m^2} \int \sin\theta \, d\theta \frac{1}{[l + R(1 - \cos\theta)]^2}, \quad (31)$$

and finally the integral over θ is easily carried out to give

$$\left\langle F_i^{(L)} F_j^{(L)} \right\rangle = \frac{\delta_{ij} g_{1s} g_{2s} R^2}{16\epsilon_0^2 \epsilon_m^2 l(l + 2R)}. \quad (32)$$

In the usual experimental setup we are in the limit where $R \gg l$, and we thus find

$$\left\langle F_i^{(L)} F_j^{(L)} \right\rangle \approx \frac{\delta_{ij} g_{1s} g_{2s} R}{32\epsilon_0^2 \epsilon_m^2 l}. \quad (33)$$

In the case where there are dielectric discontinuities we can try to approximate the computation of the force correlator in a manner similar to the proximity force approximation for electrostatic and Casimir interaction problems. When the charge distribution are delta-correlated we can assume that the force due to the interaction of a unit of area on the sphere at the same separation from the plane (thus a ring on the sphere)

is statistically independent of the others. The ring is specified by the polar angle θ, and using Eq. (22) we can write that the force on a ring of polar angle between θ and $\theta + \delta\theta$ is given by

$$F_i^{(L)}(\theta) = \left(-\frac{g_{1s} g_{2s} \epsilon_m^2}{4\pi \epsilon_0^2 (\epsilon_m + \epsilon_1)^2 (\epsilon_m + \epsilon_2)^2 \Delta_1 \Delta_2} \ln(1 - \Delta_1 \Delta_2) \right.$$
$$\left. \times \frac{\mu_i(\theta)\sqrt{2\pi R^2 \sin\theta \delta\theta}}{l + R(1 - \cos\theta)} \right)^{1/2}, \quad (34)$$

where all the prefactors $\mu(\theta)$ are independent and are of zero mean and variance one. The correlation function of the total force is thus given by

$$\left\langle F_i^{(L)} F_j^{(L)} \right\rangle = \frac{g_{1s} g_{2s} \delta_{ij} \epsilon_m^2}{4\pi \epsilon_0^2 (\epsilon_m + \epsilon_1)^2 (\epsilon_m + \epsilon_2)^2 \Delta_1 \Delta_2} \ln$$
$$\times (1 - \Delta_1 \Delta_2) \int \frac{2\pi R^2 \sin\theta \, d\theta}{[l + R(1 - \cos\theta)]^2}, \quad (35)$$

which gives

$$\left\langle F_i^{(L)} F_j^{(L)} \right\rangle = -\frac{\delta_{ij} g_{1s} g_{2s} \epsilon_m^2}{\epsilon_0^2 (\epsilon_m + \epsilon_1)^2 (\epsilon_m + \epsilon_2)^2 \Delta_1 \Delta_2} \ln$$
$$\times (1 - \Delta_1 \Delta_2) \frac{R^2}{l(l + 2R)}, \quad (36)$$

and clearly corresponds to the exact result (32) in the case where there are no dielectric discontinuities.

III. NORMAL FORCE FLUCTUATIONS

The magnitude of the normal force has been obtained previously [7,8], and we concentrate our efforts to its fluctuations. The calculations for the normal forces between dielectric slabs with random surface charging are slightly different to those for lateral forces. Here we proceed by writing the electrostatic energy as

$$E = \frac{1}{2} \int d\mathbf{x} d\mathbf{y} \rho(\mathbf{x}) G(\mathbf{x}, \mathbf{y}; l) \rho(\mathbf{y}), \quad (37)$$

where we have made explicit the dependence of the Green's function on the slab separation l. The electrostatic component of the force of the slabs in the normal direction is then given by

$$F^{(N)} = \frac{1}{2} \int d\mathbf{x} d\mathbf{y} \rho(\mathbf{x}) H(\mathbf{x}, \mathbf{y}; l) \rho(\mathbf{y}),$$
$$\text{where} \quad H(\mathbf{x}, \mathbf{y}, l) = -\frac{\partial}{\partial l} G(\mathbf{x}, \mathbf{y}; l). \quad (38)$$

The average value of the normal force is nonzero due to the correlation between the charges in each plate and their image charges [7]. In terms of the notations introduced earlier we find

$$\left\langle F^{(N)} \right\rangle = -\frac{A}{4\pi} \int k \, dk [g_{1s} \tilde{H}(k; 0, 0) \tilde{C}_1(k)$$
$$+ g_{2s} \tilde{H}(k; l, l) \tilde{C}_2(k)]. \quad (39)$$

These two terms are the interaction of the charges on surface 1 and 2 with their images. Note that the contribution of the two surfaces is additive because they are independent.

In the case where there is electrolyte in the region between the two plates that can be described on the Debye-Hückel level, one again obtains the relevant expressions for the Green's functions as

$$\tilde{G}(k;0,0) = \frac{1}{\epsilon_0(K\epsilon_m + k\epsilon_1)}\left[\frac{1 - \Delta_{1\kappa}\exp(-2Kl)}{1 - \Delta_{1\kappa}\Delta_{2\kappa}\exp(-2Kl)}\right],$$
(40)

$$\tilde{G}(k;l,l) = \frac{1}{\epsilon_0(K\epsilon_m + k\epsilon_2)}\left[\frac{1 - \Delta_{2\kappa}\exp(-2Kl)}{1 - \Delta_{1\kappa}\Delta_{2\kappa}\exp(-2Kl)}\right], \quad (41)$$

and this then gives the corresponding derivatives $\tilde{H}$ as

$$\tilde{H}(k;0,0) = \frac{4K^2\epsilon_m\Delta_{2\kappa}\exp(-2Kl)}{\epsilon_0(K\epsilon_m + k\epsilon_1)^2[1 - \Delta_{1\kappa}\Delta_{2\kappa}\exp(-2Kl)]^2},$$
(42)

$$\tilde{H}(k;l,l) = \frac{4K^2\epsilon_m\Delta_{1\kappa}\exp(-2Kl)}{\epsilon_0(K\epsilon_m + k\epsilon_2)^2[1 - \Delta_{1\kappa}\Delta_{2\kappa}\exp(-2Kl)]^2},$$
(43)

$$\tilde{H}(k;0,l)$$
$$= -\frac{2K^2\epsilon_m\exp(-Kl)[1 + \Delta_{1\kappa}\Delta_{2\kappa}\exp(-2Kl)]}{\epsilon_0(K\epsilon_m + k\epsilon_1)(K\epsilon_m + k\epsilon_2)[1 - \Delta_{1\kappa}\Delta_{2\kappa}\exp(-2Kl)]^2}.$$
(44)

The definition of $\Delta_{\alpha\kappa}$ is given in Eq. (28). The normal force fluctuations may be computed using Wick's theorem and are given by

$$\langle F^{(N)2}\rangle_c = \frac{A}{4\pi}\int k\,dk\big[g_{1s}^2\tilde{H}^2(k;0,0)\tilde{C}_1^2(k)$$
$$+ g_{2s}^2\tilde{H}^2(k;l,l)\tilde{C}_2^2(k)$$
$$+ 2g_{1s}g_{2s}\tilde{H}^2(k;0,l)\tilde{C}_1(k)\tilde{C}_2(k)\big]. \quad (45)$$

The first two terms are the force fluctuations due to the self-interactions, i.e., of the charges on surfaces 1 and 2 with their images, and the last term is the fluctuations of the force between the charges on surface 1 with those on surface 2 (whose average is always zero).

If we consider the limiting case where the intervening medium is a simple dielectric devoid of any electrolyte, i.e., $\kappa = 0$, and where the surface charges are not spatially correlated so that $C_\alpha(\mathbf{r} - \mathbf{r}') = \delta(\mathbf{r} - \mathbf{r}')$, we find that the average value of the normal force is given by

$$\langle F^{(N)}\rangle = \frac{A\epsilon_m\ln(1 - \Delta_1\Delta_2)}{4\pi\epsilon_0 l^2}$$
$$\times \left[\frac{g_{1s}}{\Delta_1(\epsilon_m + \epsilon_1)^2} + \frac{g_{2s}}{\Delta_2(\epsilon_m + \epsilon_2)^2}\right], \quad (46)$$

which recovers our previous results for the average of the normal force due to quenched charge disorder [7,8]. This result may be rewritten as

$$\langle F^{(N)}\rangle \equiv \frac{Ag_{1s}}{4\pi\epsilon_0\epsilon_m l^2}\mathcal{G}\left(\frac{\epsilon_1}{\epsilon_m}, \frac{\epsilon_2}{\epsilon_m}, \frac{g_{2s}}{g_{1s}}\right), \quad (47)$$

where the function $\mathcal{G}(\epsilon_1/\epsilon_m, \epsilon_2/\epsilon_m, g_{2s}/g_{1s})$ follows directly from Eq. (46) and is shown in Fig. 4 for the case with $g_{1s} = g_{2s}$. Note that in this case the average normal force changes
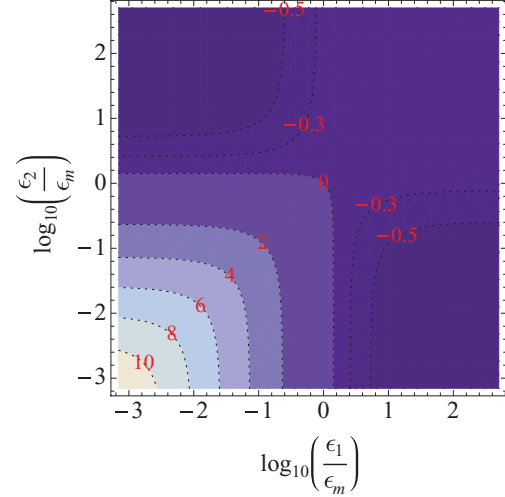

FIG. 4. (Color online) Contour plot of the rescaled normal mean force, $\mathcal{G}(\epsilon_1/\epsilon_m, \epsilon_2/\epsilon_m, g_{2s}/g_{1s})$ [Eqs. (46) and (47)], between two parallel slabs carrying quenched charge disorder with $g_{2s} = g_{1s}$ as a function of ϵ_1/ϵ_m and ϵ_2/ϵ_m shown here on a $\log_{10}$–$\log_{10}$ scale.

sign and turns from repulsive to attractive when ϵ_1/ϵ_m and ϵ_2/ϵ_m become larger than a certain value (shown in the figure by the contour line labeled with 0). For the symmetric case with $\Delta_1 = \Delta_2 = \Delta$, one has an attractive force when $\Delta > 0$ (e.g., for two dielectric slabs interacting across vacuum) and a repulsive force when $\Delta < 0$. The normal force tends to zero when both dielectric constants ϵ_1 and ϵ_2 go to infinity (perfect metal limit) and diverges logarithmically when both ϵ_1/ϵ_m and $\epsilon_2/\epsilon_m \to 0$. The force can take a finite limiting value when one of the dielectric constants is set to zero and the other one tends to infinity, e.g., $\mathcal{G}(x,0) \to -\ln 2 \simeq -0.69$ when $x \to \infty$.

In this case the normal force fluctuations variance $\langle F^{(N)2}\rangle_c = \langle F^{(N)2}\rangle - \langle F^{(N)}\rangle^2$ are given by

$$\langle F^{(N)2}\rangle_c = \frac{A}{4\pi\epsilon_0^2\epsilon_m^2 l^2}\left(g_{1s}^2 D_{11} + g_{2s}^2 D_{22} + 2g_{1s}g_{2s}D_{21}\right),$$
(48)

where

$$D_{11} = \frac{2\epsilon_m^4}{3(\epsilon_m + \epsilon_1)^4}\left[\frac{\Delta_2}{\Delta_1(1 - \Delta_1\Delta_2)^2} + \frac{\ln(1 - \Delta_1\Delta_2)}{\Delta_1^2}\right],$$
(49)

$$D_{22} = \frac{2\epsilon_m^4}{3(\epsilon_m + \epsilon_2)^4}\left[\frac{\Delta_1}{\Delta_2(1 - \Delta_1\Delta_2)^2} + \frac{\ln(1 - \Delta_1\Delta_2)}{\Delta_2^2}\right],$$
(50)

$$D_{21} = \frac{\epsilon_m^4}{3(\epsilon_m + \epsilon_1)^2(\epsilon_m + \epsilon_2)^2}\left[-\frac{1}{\Delta_1\Delta_2}\ln(1 - \Delta_1\Delta_2)\right.$$
$$\left.+ \frac{2}{(1 - \Delta_1\Delta_2)^2}\right].$$
(51)

These expressions for D_{11} and D_{21} are shown in Figs. 5a and b as a function of ϵ_1/ϵ_m and ϵ_2/ϵ_m (note that D_{22} can be obtained from D_{11} by replacing the subindex 1 with 2 and vice versa). In Fig. 5c, we show the quantity $D_{11} + D_{22} + 2D_{21}$, which
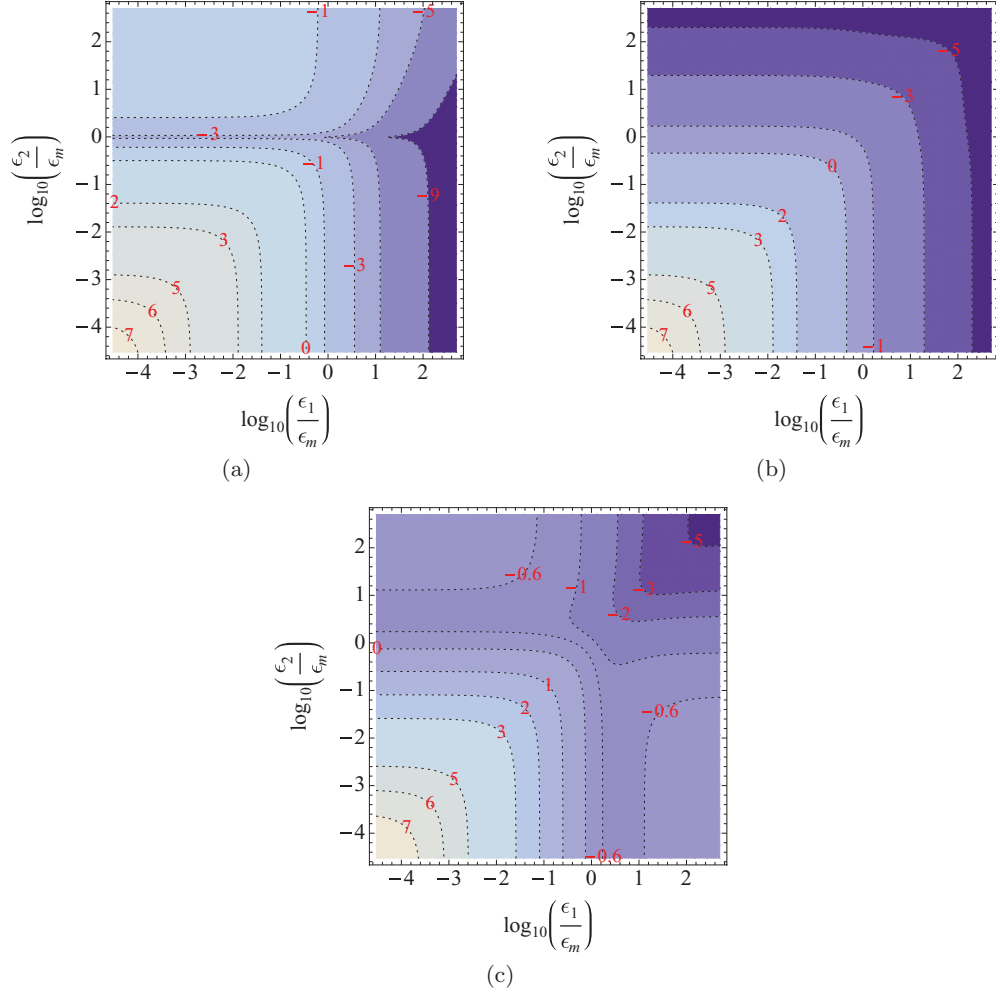
(a)

(b)

(c)

FIG. 5. (Color online) Contour plots of (a) $\log_{10} D_{11}$, the contribution to the force fluctuations due to the self interactions, i.e., of the charges on surface 1 with their images, and (b) $\log_{10} D_{21}$, the contribution to the force fluctuations due to the interaction between the charges on surface 1 with those on surface 2 as a function of ϵ_1/ϵ_m and ϵ_2/ϵ_m. (c) The rescaled normal force fluctuations $\log_{10} \mathcal{L}(\epsilon_1/\epsilon_m, \epsilon_2/\epsilon_m, g_{2s}/g_{1s})$ for $g_{1s} = g_{2s}$. All plots are shown in a $\log_{10}$–$\log_{10}$ scale for ϵ_1/ϵ_m and ϵ_2/ϵ_m.

can be defined to be the rescaled normal force fluctuations for the case with $g_{1s} = g_{2s}$ through

$$\langle F^{(N)2}\rangle_c \equiv \frac{Ag_{1s}^2}{4\pi\epsilon_0^2\epsilon_m^2 l^2}\mathcal{L}\left(\frac{\epsilon_1}{\epsilon_m}, \frac{\epsilon_2}{\epsilon_m}, \frac{g_{2s}}{g_{1s}}\right). \quad (52)$$

The different contributions $D_{\alpha\beta}$ to the normal force fluctuations all diverge algebraically when $\epsilon_\alpha/\epsilon_m \to 0$, i.e., $\mathcal{L}(x,x) \sim x^{-2}$ when $x \to 0$.

In the case where there are no dielectric discontinuities, the forces due to image charges are zero, and the only normal force is due to the interaction between the charges on the two (net-neutral) surfaces [one can easily see that $D_{11} = 0$ when $\epsilon_2/\epsilon_m = 1$; the same is true for $D_{22} = 0$ when $\epsilon_1/\epsilon_m = 1$, which explains the nonmonotonic behavior of D_{11} and $\mathcal{L}(\epsilon_1/\epsilon_m, \epsilon_2/\epsilon_m, 1)$ as seen in Fig. 5a and c]. The mean of the normal force is clearly zero in this case, but it has a nonzero variance

$$\langle F^{(N)2}\rangle_c = \frac{Ag_{1s}g_{2s}}{32\pi\epsilon_0^2\epsilon_m^2 l^2}, \quad (53)$$

a result that can be verified using the expression for the Coulomb potential in a system of constant dielectric constant ϵ_m, with a computation similar to that leading to Eq. (A4) and then Eq. (25). Interestingly we see, comparing with Eq. (25), that in the case of a uniform dielectric constant the variance of the force fluctuations in the normal direction is twice the magnitude as those in the lateral direction.

A. PFA for normal forces

Within the proximity force approximation for the sphere-plane geometry in complete analogy to the case of lateral force we can derive both the normal force as well as its fluctuations. The former can be obtained in the form

$$\langle F^{(N)}\rangle = \frac{R^2\epsilon_m \ln(1 - \Delta_1\Delta_2)}{\epsilon_0 l(l + 2R)}\left[\frac{g_{1s}}{\Delta_1(\epsilon_m + \epsilon_1)^2}\right.$$
$$\left. + \frac{g_{2s}}{\Delta_2(\epsilon_m + \epsilon_2)^2}\right], \quad (54)$$

and the normal force fluctuations as

$$
\langle F^{(N)2}\rangle_c = \frac{R^2}{\epsilon_0^2 \epsilon_m^2 l(l+2R)} \big(g_{1s}^2 D_{11} + g_{2s}^2 D_{22} \\
+ 2g_{1s}g_{2s}D_{21}\big). \tag{55}
$$

From this formula we see that the relative size of the fluctuations of the normal force to its average scales as

$$
\frac{\sqrt{\langle F^{(N)2}\rangle_c}}{\langle F^{(N)}\rangle} \sim \sqrt{\frac{l(l+R)}{R^2}}, \tag{56}
$$

and thus the fluctuations of the normal force relative to its average value become more important as the separation is increased! In other words, the sample-to-sample scatter in the normal force increases on increasing the separation between the interacting bodies. This could be interpreted to mean that the interactions themselves restrict their own fluctuations.

IV. CONCLUSIONS

In this work we have proven that the sample-to-sample variance in the lateral as well as normal charge disorder-generated forces can be substantial. In the ideal (thermodynamic type) limit where the probe area is very large the force is much larger than its fluctuations. However, in some experimental setups the probe size may be quite small, and so sample-to-sample force fluctuations could become important with respect to average forces. In addition, we have shown that, for the sphere-plane setup, fluctuations become important at large separations where the normal force is weak. In the case of lateral force variance, since the average is zero, the fluctuations are the only thing remaining. Interestingly enough, the fluctuations in the normal and lateral directions are always comparable. For the special case of a uniform dielectric constant we also showed that the variance of the force fluctuations in the normal direction is exactly twice the magnitude of the one in the lateral direction.

The sample-to-sample variation in the disorder-generated force is fundamentally different from the thermal force fluctuations in (pseudo-) Casimir interactions as analyzed by Bartolo *et al.* [17]. In this case one could (in principle at least) use the same experimental setup and just observe the temporal variation of the force at a certain position of the interacting surfaces, measuring the average and the variance within the same experiment (assuming a sufficiently good temporal resolution of the force-measuring apparatus). Additionally, the variance of the fluctuation-induced Casimir force is not universal and is intrinsically related to the microscopic physics that governs the interaction between the fluctuating (elastic in the case investigated in Ref. [17]) field and the bounding surfaces. On the other hand, in order to detect sample-to-sample variation one would have to perform many experiments and then look at the variation in the measured force between them. In the first case, the variance of the force is intrinsic to the field fluctuations; in the second one, it is intrinsic to the material properties of the interacting bodies. We should emphasize here that the quenched nature of the charge distribution is crucial to much of the physics discussed in this paper. When charge distributions are annealed, charges can rearrange themselves to lower the free energy of the system, and the resulting interactions are very different [7,8] and sample-to-sample fluctuations will not exist. However, fluctuations in the annealed charge distribution should lead to thermal force fluctuations of the type discussed in Ref. [17]. It should be reiterated that electrostatic potential disorder exists even at metallic surfaces due to the patch effect [4,5], although the resulting interaction is of a shorter range than that coming from quenched charge disorder.

There are several assumptions in our calculation that need to be spelled out explicitly. We always assume that the position and orientation of the interacting surfaces are fixed in these experiments as well as in the corresponding calculation, just as indicated in the schematic representation of our system on Fig. 1. However, for an unconstrained colloid particle rotational degrees of freedom are not quenched but rather annealed. For example, a spherical colloid will rotate so as to minimize its interaction energy in the same way as permanent dipoles orientate with each other. This would introduce additional considerations in the analysis of forces that we do not address in this contribution. In principle there will be random torques, and their sample-to-sample variation can be computed using the same methods as presented here. These random torques may be accessible to torsion-balance-based setups [21]. Additionally, in force measurements, slight translations of the sphere with respect to the plane and slight rotations of the sphere will lead to different measurements for both normal and lateral forces as well as their fluctuations.

APPENDIX: DIRECT CALCULATION OF LATERAL FORCE FLUCTUATIONS FOR TWO SLABS WITH $\epsilon_2 = \epsilon_1 = \epsilon_m$

Let us consider the lateral force fluctuations in the slab system in the absence of dielectric discontinuities, i.e., when $\epsilon_2 = \epsilon_1 = \epsilon_m$. Here we can use the method used in Ref. [12] to analyze the statistics of the potential between two randomly charged sheets (with no dielectric discontinuity), which can easily be adapted to study force fluctuations. The standard three-dimensional Coulomb interaction can be written as

$$
E = \frac{1}{2}\int d\mathbf{x}\,d\mathbf{y}\,\frac{\rho(\mathbf{x})\rho(\mathbf{y})}{4\pi\epsilon_0\epsilon_m[(\mathbf{x}-\mathbf{y})^2 + l^2]^{\frac{1}{2}}}, \tag{A1}
$$

and the change in energy is thus

$$\delta E = \int d\mathbf{x}\, d\mathbf{y}\, \frac{\mathbf{a} \cdot \boldsymbol{\nabla} \rho_1(\mathbf{x}) \rho_2(\mathbf{y})}{4\pi \epsilon_0 \epsilon_m [(\mathbf{x} - \mathbf{y})^2 + l^2]^{\frac{1}{2}}}. \qquad \text{(A2)}$$

The average value of δE is clearly zero, but one can show that for delta-correlated charge distributions

$$\langle \delta E^2 \rangle = \frac{g_{1s} g_{2s}}{16\pi^2 \epsilon_0^2 \epsilon_m^2} \int d\mathbf{x}\, d\mathbf{y}\, \frac{[\mathbf{a} \cdot (\mathbf{x} - \mathbf{y})]^2}{[(\mathbf{x} - \mathbf{y})^2 + l^2]^3}. \qquad \text{(A3)}$$

From this one can extract the force correlator as

$$\langle F_i^{(L)} F_j^{(L)} \rangle = \frac{\delta_{ij} g_{1s} g_{2s}}{32\pi^2 \epsilon_0^2 \epsilon_m^2} A \int d\mathbf{z}\, \frac{\mathbf{z}^2}{(\mathbf{z}^2 + l^2)^3}, \qquad \text{(A4)}$$

where the integral over $\mathbf{z}$ is over the relative position $\mathbf{x} - \mathbf{y}$, and the leading-order term is proportional to A (there will be a correction term proportional to the perimeter ∂A of the region containing the charge on plate 1). The integral in Eq. (A4) is then easily evaluated to recover the result (25).

---

[1] R. French *et al.*, Rev. Mod. Phys. **82**, 1887 (2010).

[2] See book review by S. K. Lamoreaux: M. Bordag, G. L. Klimchitskaya, U. Mohideen, and V. M. Mostepanenko, *Advances in the Casimir Effect* (Oxford University Press, New York, 2009) in *Physics Today*, August 2010.

[3] W. J. Kim, M. Brown-Hayes, D. A. R. Dalvit, J. H. Brownell, and R. Onofrio, Phys. Rev. A **78**, 020101(R) (2008); **79**, 026102 (2009); W. J. Kim, A. O. Sushkov, D. A. R. Dalvit, and S. K. Lamoreaux, Phys. Rev. Lett. **103**, 060401 (2009); R. S. Decca, E. Fischbach, G. L. Klimchitskaya, D. E. Krause, D. Lopez, U. Mohideen, and V. M. Mostepanenko, Phys. Rev. A **79**, 026101 (2009); S. de Man, K. Heeck, and D. Iannuzzi, *ibid.* **79**, 024102 (2009).

[4] C. C. Speake and C. Trenkel, Phys. Rev. Lett. **90**, 160403 (2003).

[5] L. F. Zagonel, N. Barrett, O. Renault, A. Bailly, M. Bäurer, M. Hoffmann, S.-J. Shih, and D. Cockayne, Surf. Interface Anal. **40**, 1709 (2008).

[6] D. S. Dean, R. R. Horgan, A. Naji, and R. Podgornik, Phys. Rev. A **79**, 040101(R) (2009); Phys. Rev. E **81**, 051117 (2010).

[7] A. Naji, D. S. Dean, J. Sarabadani, R. R. Horgan, and R. Podgornik, Phys. Rev. Lett. **104**, 060601 (2010).

[8] J. Sarabadani, A. Naji, D. S. Dean, R. R. Horgan, and R. Podgornik, J. Chem. Phys. **133**, 174702 (2010).

[9] A. Naji and R. Podgornik, Phys. Rev. E **72**, 041402 (2005); R. Podgornik and A. Naji, Europhys. Lett. **74**, 712 (2006); Y. S. Mamasakhlisov, A. Naji, and R. Podgornik, J. Stat. Phys. **133**, 659 (2008).

[10] E. E. Meyer, Q. Lin, T. Hassenkam, E. Oroudjev, and J. N. Israelachvili, Proc. Natl. Acad. Sci. USA **102**, 6839 (2005); S. Perkin, N. Kampf, and J. Klein, Phys. Rev. Lett. **96**, 038301 (2006); J. Phys. Chem. B **109**, 3832 (2005); E. E. Meyer, K. J. Rosenberg, and J. Israelachvili, Proc. Natl. Acad. Sci. USA **103**, 15739 (2006).

[11] Y. Kantor, H. Li, and M. Kardar, Phys. Rev. Lett. **69**, 61 (1992); I. Borukhov, D. Andelman, and H. Orland, Eur. Phys. J. B **5**, 869 (1998).

[12] S. Panyukov and Y. Rabin, Phys. Rev. E **56**, 7053 (1997).

[13] L. I. Daikhin and M. Urbakh, Phys. Rev. E **59**, 1921 (1999).

[14] D. B. Lukatsky, K. Zedovich, and E. I. Shakhnovich, Phys. Rev. Lett . **97**, 178101 (2006); D. B. Lukatsky and E. I. Shakhnovich, Phys. Rev. E **77**, 020901(R) (2008).

[15] J Israelachvili *et al.*, Rep. Prog. Phys. **73**, 036601 (2010).

[16] U. Raviv and J. Klein, Science **297**, 1540 (2002).

[17] D. Bartolo, A. Ajdari, J. B. Fournier, and R. Golestanian, Phys. Rev. Lett. **89**, 230601 (2002).

[18] H.-J. Butt and M. Kappl, *Surface and Interfacial Forces* (Wiley-VCH, New York, 2010).

[19] N. V. Churaev, B. V. Derjaguin, and V. M. Muller, *Surface Forces* (Springer, New York, 1987).

[20] M. Kanduvc, A. Naji, J. Forsman, and R. Podgornik, J. Chem. Phys. **132**, 124701 (2010).

[21] A. Lambrecht, V. V. Nesvizhevsky, R. Onofrio, and S. Reynaud, Class. Quantum Grav. **22**, 5397 (2005).